Supplementary material for:

# In-situ high-energy X-ray diffraction study of austenite decomposition during rapid cooling and isothermal holding in two HSLA steels

Sen Lin [a*], Ulrika Borggren [b], Andreas Stark [c], Annika Borgenstam [a], Wangzhong Mu [a], Peter Hedström [a]

[a] Department of Materials Science and Engineering, KTH Royal Institute of Technology, Stockholm, SE-10044, Sweden

[b] SSAB AB, Borlänge, SE-78184, Sweden

[c] Helmholtz Zentrum Geesthacht, Institute of Materials Research, Max Planck Straße 1, 21502 Geesthacht, Germany

[*] Corresponding author: senlin@kth.se

Since the austenite decomposition occurs at relatively high temperatures, the possibility of substitutional elements diffusion should be examined. Therefore, energy-dispersive X-ray spectroscopy (EDS) analysis are performed using a field-emission scanning electron microscope JEOL 7800F. The detailed sample preparation procedure and EDS analysis configuration is described in the main text of the article. Both point detection and area mapping are used to quantify the chemical composition of the substitutional elements in different microstructure constituents, including bainite, polygonal ferrite, and martensite/austenite constituents.

The microstructure and the distribution of the major alloying elements (Mn, Si, Cr) for LCE550 and HCE550 are shown in Fig. S1 and Fig. S2, respectively. The positions of the point detection are shown as red dots in Fig. S1 (a) and Fig. S2 (a). The EDS mapping of Mn, Si, Cr shows little redistribution (Fig. S1 (b-d) and Fig. S2 (b-d).). The normalized mass concentration obtained from point detection and area mapping are listed in Table S1. The chemical composition detected in different locations are all close to the nominal composition of the materials. EDS analysis is also performed on other samples (LCE450, HCE450) and similar results are obtained. Therefore, it can be concluded that during the entire austenite decomposition process, the substitutional elements remained homogeneous and their effect on lattice parameter variation can be neglected.

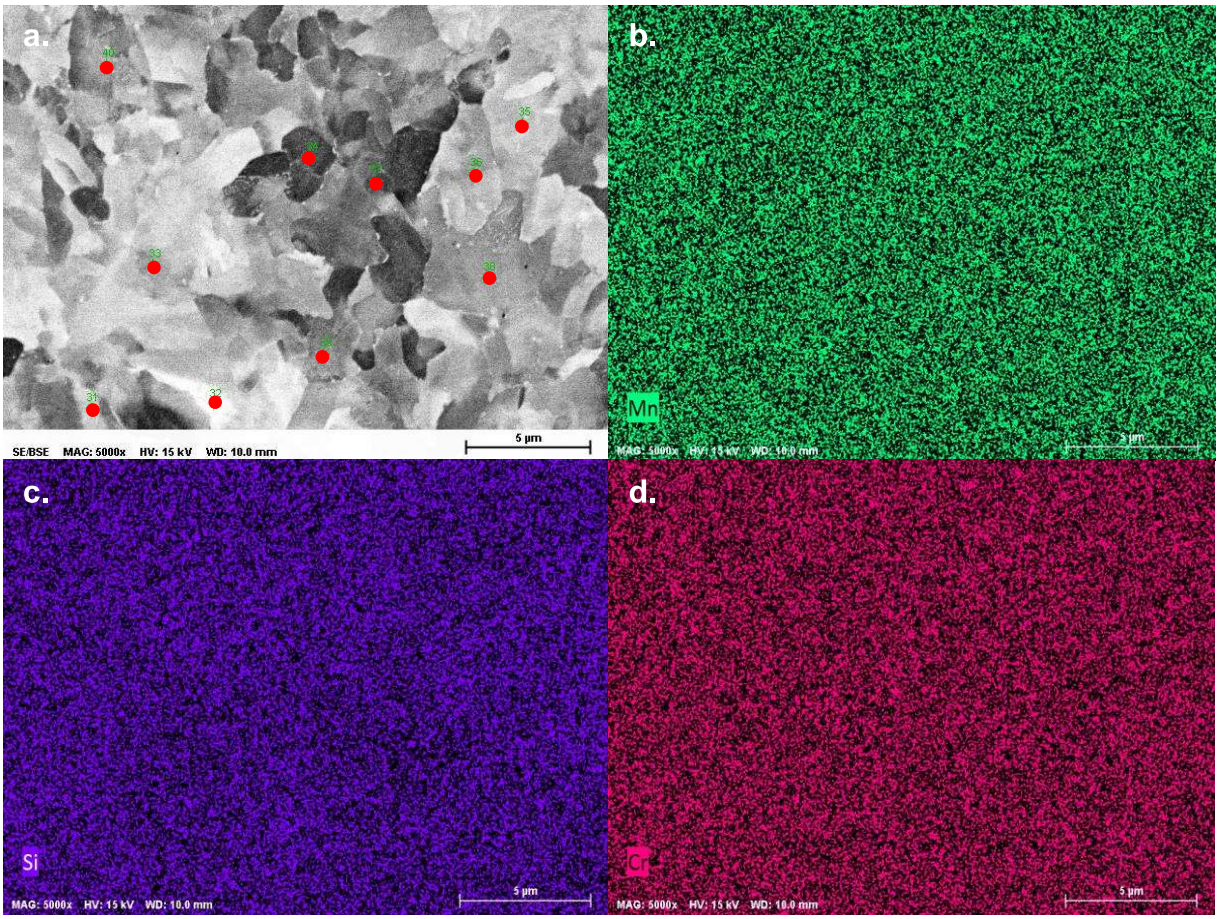


*Fig. S-1 EDS analysis on LCE550. The microstructure is shown in (a.), the red dots are the locations for point detections; major element mapping for (b.) Mn; (c.) Si; (d.) Cr show homogeneous distribution after the heat treatment.*

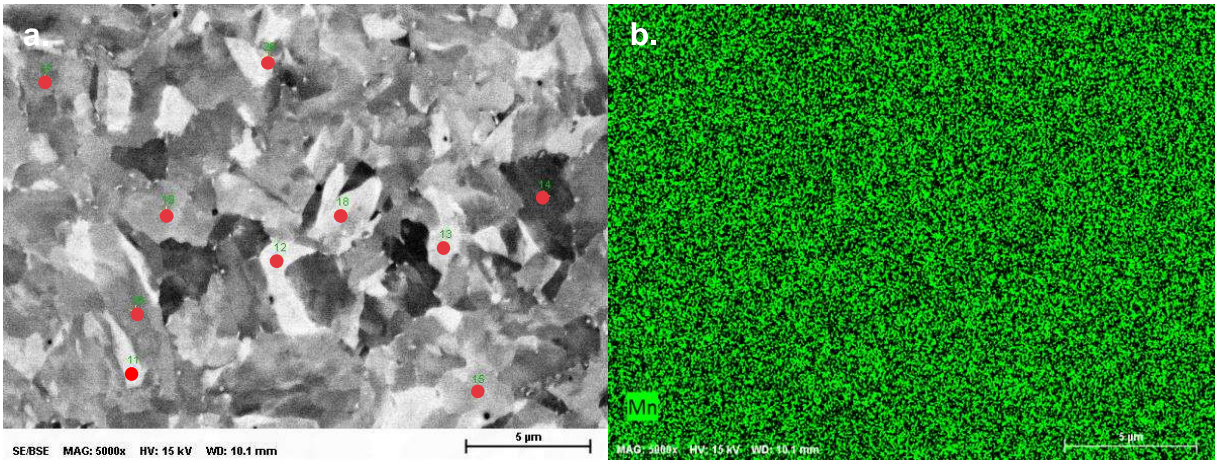

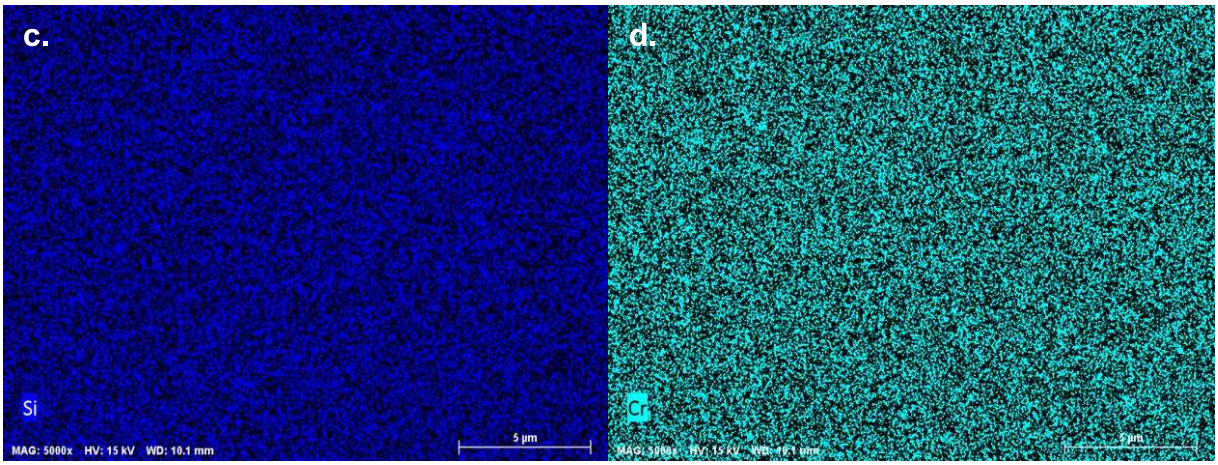


*Fig. S-2 EDS analysis on HCE550. The microstructure is shown in (a.), the red dots are the locations for point detections; major element mapping for (b.) Mn; (c.) Si; (d.) Cr show homogeneous distribution after the heat treatment.*

*Table S-I The normalized mass percent (wt%) of the major elements obtained from EDS mapping and point detection. The representative values in point detection is from one (out of ten) detection position.*

| | Mn | Si | Cr | Ni | Mo | Cu |
|---|---|---|---|---|---|---|
| LCE550-Mapping | 2.12 | 0.49 | 0.32 | 0.19 | 0.01 | 0.04 |
| LCE550-Point | 2.06 | 0.46 | 0.32 | 0.15 | 0.03 | 0.05 |
| HCE550-Mapping | 2.09 | 0.28 | 0.73 | 0.05 | 0.08 | 0.12 |
| HCE550-Point | 2.10 | 0.22 | 0.75 | 0.06 | 0.05 | 0.14 |

DICTRA simulation is performed to illustrate the influence of chemical composition on the transformation kinetics of polygonal ferrite during quenching. The simulation procedure is described in the main text of the article, but with different selection of alloying elements. The transformation condition is negligible partitioning local equilibrium. Fig. S-3 (a) shows that the transformation kinetics for polygonal ferrite in HCE450 and LCE450 would be similar when only considering C, Mn, Si, Cr alloy addition, indicating that the difference in Si and Cr addition between the two alloys cannot account for the observed transformation kinetics difference. Fig. S-3 (b) shows the transformation kinetics when inputting Nb and Mo in HCE450. The kinetics is similar between the simulation with Nb input and without. And there is a clear retardation on the transformation kinetics when Mo is considered in the simulation.

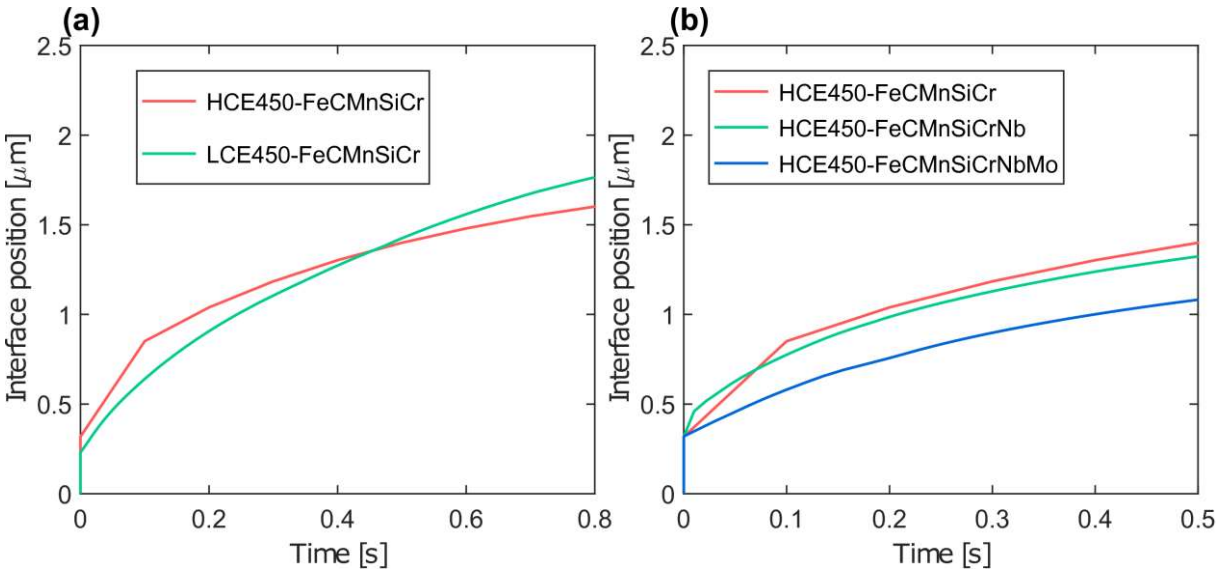


*Fig. S-3 The DICTRA simulation of polygonal ferrite formation under negligible partitioning local equilibrium. The interface position indicates the kinetics of the transformation. (a.) simulation with input of alloying addition of C, Mn, Si, Cr for HCE450 and LCE450; (b.) simulation with input of alloying addition of C, Mn, Si, Cr, Nb, and Mo for HCE450.*

Fig. S-4 shows the concentration profiles of C and Mn across the interface for HCE450, HCE550, LCE450, and LCE550 obtained from the same DICTRA simulations under local equilibrium condition (same simulation mentioned in the main text). The concentration profiles for Mn indicate negligible partitioning local equilibrium. Fig. S-5 shows the concentration profiles of C and Mn across the interface for HCE450, HCE550, LCE450, and LCE550 under paraequilibrium (same simulation mentioned in the main text).

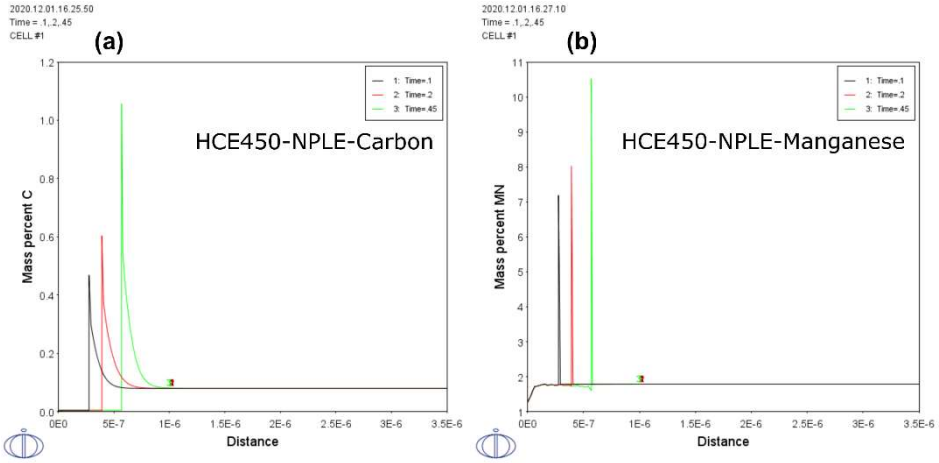
2020.12.01.16.25.50
Time = .1,.2,.45
CELL #1
(a)
HCE450-NPLE-Carbon
Mass percent C
Distance
1: Time=.1
2: Time=.2
3: Time=.45


2020.12.01.16.27.10
Time = .1,.2,.45
CELL #1
(b)
HCE450-NPLE-Manganese
Mass percent MN
Distance
1: Time=.1
2: Time=.2
3: Time=.45

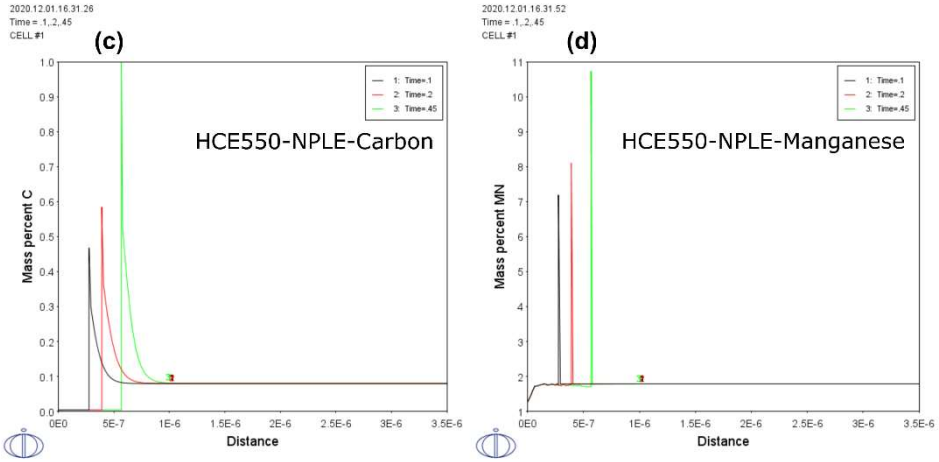
2020.12.01.16.31.26
Time = .1,.2,.45
CELL #1
(c)
HCE550-NPLE-Carbon
Mass percent C
Distance
1: Time=.1
2: Time=.2
3: Time=.45


2020.12.01.16.31.52
Time = .1,.2,.45
CELL #1
(d)
HCE550-NPLE-Manganese
Mass percent MN
Distance
1: Time=.1
2: Time=.2
3: Time=.45

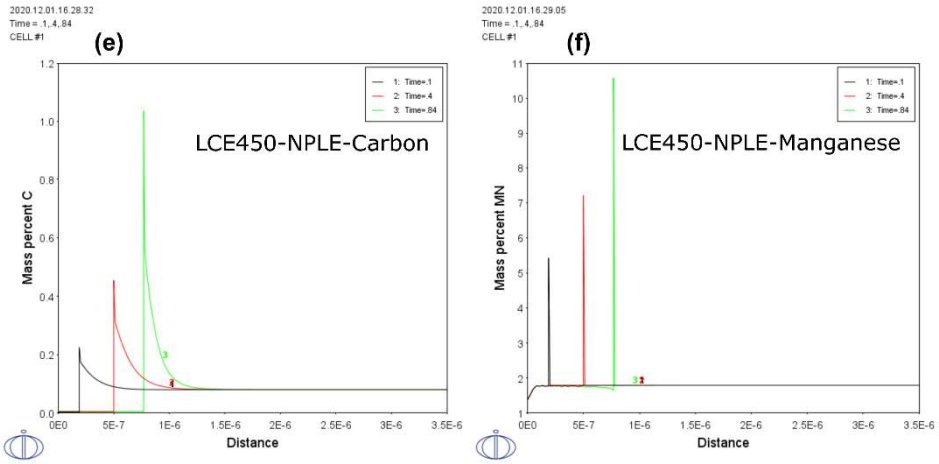
2020.12.01.16.28.32
Time = .1,.4,.84
CELL #1
(e)
LCE450-NPLE-Carbon
Mass percent C
Distance
1: Time=.1
2: Time=.4
3: Time=.84


2020.12.01.16.29.05
Time = .1,.4,.84
CELL #1
(f)
LCE450-NPLE-Manganese
Mass percent MN
Distance
1: Time=.1
2: Time=.4
3: Time=.84

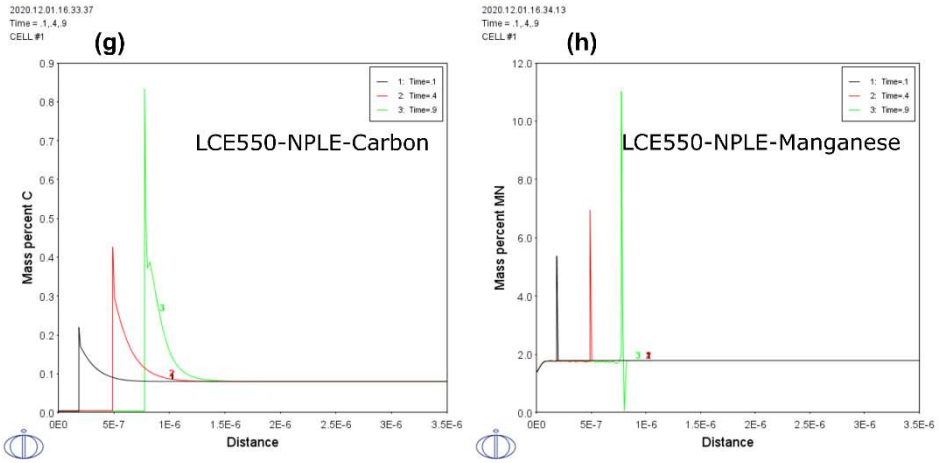
2020.12.01.16.33.37
Time = .1,.4,.9
CELL #1
(g)
LCE550-NPLE-Carbon
Mass percent C
Distance
1: Time=.1
2: Time=.4
3: Time=.9


2020.12.01.16.34.13
Time = .1,.4,.9
CELL #1
(h)
LCE550-NPLE-Manganese
Mass percent MN
Distance
1: Time=.1
2: Time=.4
3: Time=.9

*Fig. S-4 Chemical concentration profiles across the interface under local equilibrium condition. (a.) (b.) concentration profiles of C and Mn in HCE450, respectively; (c.) (d.) concentration profiles of C and Mn in HCE550, respectively; (e.) (f.) concentration profiles of C and Mn in LCE450, respectively; (g.) (h.) concentration profiles of C and Mn in LCE550, respectively.*

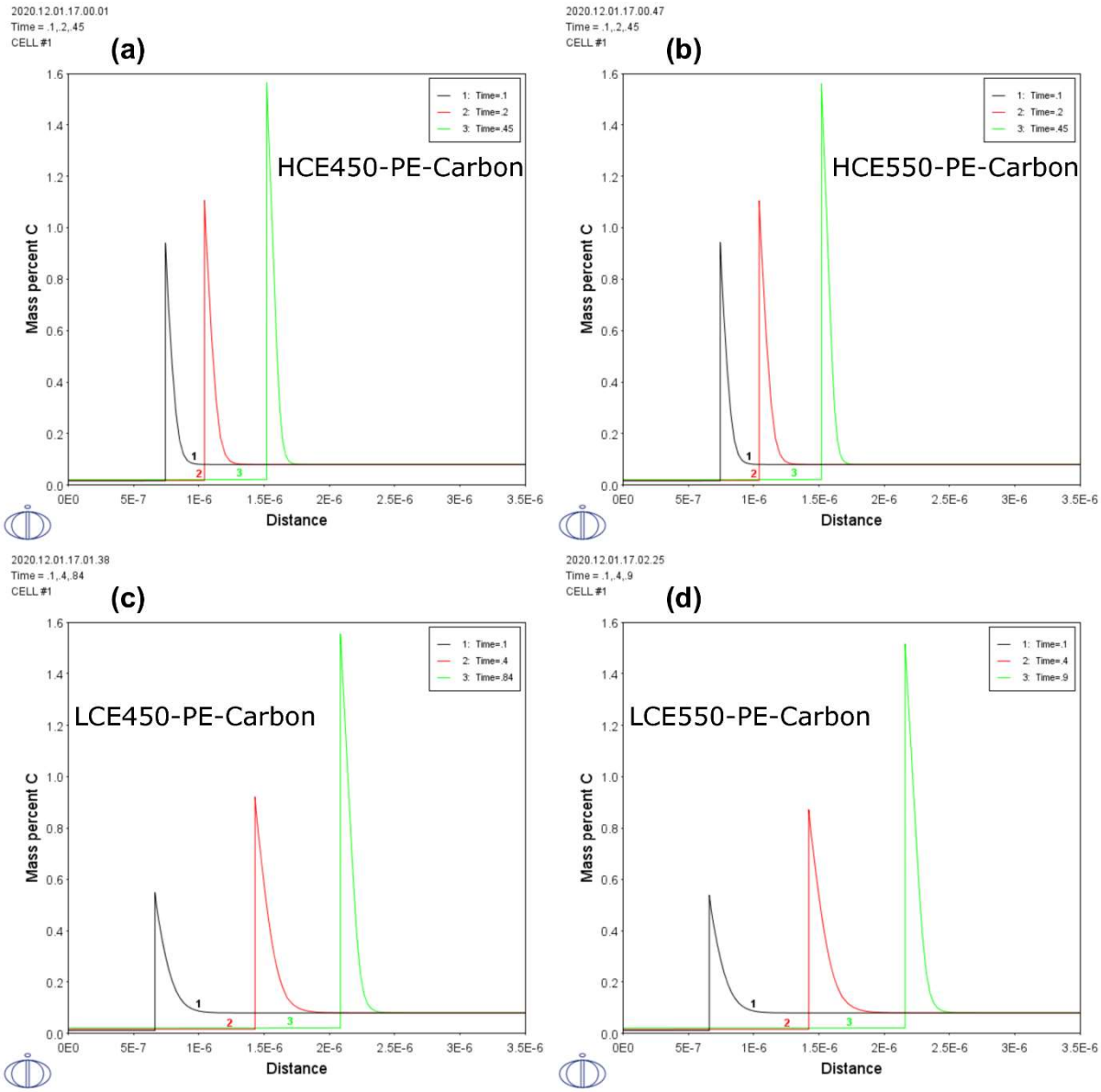


*Fig. S-5 Carbon concentration profiles across the interface under para equilibrium condition. (a.) for HCE450, (b.) for HCE550, (c.) for LCE450, (d.) for LCE550.*